

ICAS PAPER
No. 72 - 09



LAMINAR AND TURBULENT BOUNDARY LAYER
STUDIES AT HYPERSONIC SPEEDS

by

J. L. Stollery, Reader in Aeronautics
Imperial College, London, U.K.

**The Eighth Congress
of the
International Council of the
Aeronautical Sciences**

INTERNATIONAAL CONGRESCENTRUM RAI-AMSTERDAM, THE NETHERLANDS
AUGUST 28 TO SEPTEMBER 2, 1972

Price: 3. Dfl.

LAMINAR AND TURBULENT BOUNDARY-LAYER
STUDIES AT HYPERSONIC SPEEDS

J.L. Stollery
Aeronautics Department, Imperial College
London, England

Abstract

The paper reports the results of theoretical and experimental boundary layer investigations relevant to the space shuttle and future hypersonic aircraft. Laminar and turbulent flows over flat plate, wedge, concave, convex and compression corner surfaces are considered, including the effects of strong viscous interaction, shock-boundary layer interaction and flow separation. Comparisons are made between the surface heat transfer and pressure measurements and predictions from the wide variety of theories now available. The conditions for incipient separation are specified and it is shown that both laminar and turbulent boundary layers become more resistant to separation as the Mach number rises.

Introduction

The flight pattern of future hypersonic vehicles is likely to be so diverse that extensive knowledge of both laminar and turbulent boundary layer growth under a variety of wall temperature and pressure gradient conditions will be required. Although only hypersonic continuum perfect gas flows are considered here, the variety of conditions range from low Reynolds number laminar flow to high Reynolds number turbulent flow. At high altitude the laminar boundary layers are so thick that their growth severely distorts the inviscid flow field which in turn modifies the pressure field in which the layer grows. Thus strong viscous interaction must be considered particularly in the neighbourhood of the leading edge. Another area in which the mutual interaction between boundary layer and the external pressure field is important is near a deflected control surface (Fig.1). For example, a positive control deflection can separate the boundary layer and significantly modify both the overall forces and the local pressure and heat transfer rate distributions.

Experiments have been performed at $M = 8$ and 12 on a variety of two-dimensional shapes in the No.1 gun tunnel to provide data not only relevant to future designs but also useful for testing the various laminar flow theories now available. The simplest of these is based on the classic work of Cheng et al.(1) which considered the separate and combined effects of incidence, leading edge thickness and boundary layer displacement. However, some of the predictions by this method are unrealistic owing to the use of the Newton-Busemann pressure law. The method has now been improved and extended by Sullivan(2) and Stollery(3)(4) to give reasonable first estimates of unseparated flow over any two-dimensional surface.

The very powerful Lees-Reeves(5) momentum integral technique, further developed by Holden(6) and Klineberg(7) for non-adiabatic wall conditions, can be used for attached, incipient and fully separated flows. It is one of the few theoretical methods capable of marching right through a fully separated flow region. Georgeff(8) has compared

predictions using this method* with a wide variety of compression corner data and extended the technique(9) to cover any value of wall temperature, either constant or varying along the chord.

A more accurate estimate of attached laminar flow with viscous interaction is to solve the boundary layer flow using one of the implicit finite difference schemes. Wornom and Werle(10) have made calculations of this type using the program developed by Flügge-Lotz and Blottner(11) with later modifications by Davis(12). Wornom and Werle use the tangent-wedge law to describe the external inviscid flow and a simple coupling equation to define the effective body shape as the geometric surface plus displacement thickness. They do, however, allow for the effects of normal pressure gradient on both the inviscid and viscous flow regions and obtain good agreement with the experimental pressure distribution measured at $M = 12$ on a concave cubic surface (see Fig.4a).

A more sophisticated and potentially more accurate estimate can be obtained by solving the external inviscid, but rotational, flow by the method of characteristics and matching it correctly to an 'exact' boundary layer calculation. Smith is currently attempting this exercise using the boundary layer program of Sells(13).

This paper includes numerous comparisons between experimental data and the various theoretical predictions.

The No.2 hypersonic gun tunnel(14) was specifically designed for turbulent boundary layer research and Reynolds numbers of 35×10^6 can be obtained at $M = 9$. Since the theory of hypersonic, non-adiabatic, turbulent boundary layers is not very well established, some flat plate measurements have been made by Coleman(15) in order to test the various semi-empirical calculation techniques. Measurements have been made in the range $3 \leq M \leq 9$ by tilting a flat plate in the Mach 9 test stream to obtain the local Mach number desired.

Since at hypersonic speeds transition Reynolds numbers are quite high $\{0[10^6]\}$ the problem of strong turbulent viscous interaction near a leading edge is unlikely to arise. However the problem of shock-boundary layer interaction is relevant to control surface deflection. The tests show that very large flap deflections are needed to separate the turbulent boundary-layer so that for most practical applications the flow will remain attached. For such flows satisfactory calculations of pressure(16) and heat transfer(17) may be possible using some quite simple prediction techniques.

Theoretical Considerations

The most general analysis must include the

*hereafter referred to as the LRHK method

combined effects of geometric shape (incidence, bluntness) and boundary layer growth. Some typical flow patterns are shown in Fig.1. The interdependent equations which must be solved either simultaneously or by iteration are:

$$y_e = f_1(y_b) \quad (1)$$

$$y_b = f_2(\delta^*) \quad (2)$$

$$\delta^* = f_3(p_e) \quad (3)$$

$$p_e = f_4(y_e) \quad (4)$$

The problem can be made either simple and approximate, or complex and accurate, depending on the choice of $f_{1,2,3,4}$ and the form of equation (3) will depend on whether the boundary layer is laminar or turbulent.

The effects of bluntness and skin friction are similar in that both generate high temperature, low density layers with negligible normal pressure gradients, which enlarge the effective body shape and so distort the external inviscid flow. A simple relationship for the entropy layer (δ_e) was derived independently by Cheng⁽¹⁾ and Chernyi⁽¹⁸⁾ in terms of the nose drag coefficient k as

$$(y_e - y_b) \left(\frac{p_e/p_\infty}{\gamma M_\infty^2} \right) = \left\{ \frac{\gamma - 1}{4} \right\} kt \quad (1a)$$

Equation (2) 'couples' the viscous and inviscid flow fields; the exact relation is

$$\frac{v_b}{u_b} = \frac{d(y_b - y_w)}{dx} = \frac{d\delta^*}{dx} - \left[1 - \frac{\delta^*}{\delta} \right] \left[\frac{d}{dx} (\log \rho_b u_b) \right] \quad (2a)$$

but at hypersonic speeds the mass in the boundary layer is so small that $\delta^* \approx \delta$ and so quite often the approximate expression

$$y_b = y_w + \delta^* \quad (2b)$$

is used instead.

The choice of an appropriate pressure law is very wide. Cheng et al.⁽¹⁾ used the Newton-Busemann relation

$$P \equiv p_e/p_\infty = \gamma M_\infty^2 (y_e'^2 + y_e''^2) \quad (4a)$$

Stollery⁽³⁾ showed that this choice could lead to unrealistic answers on concave surfaces and following Sullivan⁽²⁾ employed the tangent wedge rule

$$P = 1 + \gamma (M_\infty y_e')^2 \left[\left(\frac{\gamma + 1}{4} \right) + \left\{ \left(\frac{\gamma + 1}{4} \right)^2 + \frac{1}{(M_\infty y_e')^2} \right\}^{\frac{1}{2}} \right] \quad (4b)$$

In the LRHK method the more exact shock expansion theory is used.

Laminar flow

The degree of sophistication in any theory is primarily dictated by the choice of f_3 in equation (3). Again Cheng et al. use one of the simplest ideas as proposed by Lees⁽¹⁹⁾, namely local

flat plate similarity, which predicts that

$$\frac{M_\infty \delta^*}{x} = \frac{A \bar{\chi}}{P} \left\{ \frac{1}{x} \int_0^x P dx \right\}^{\frac{1}{2}} \quad (3a)$$

Lees showed that at least for cold wall flows the boundary layer equations could be transformed and reduced to the Blasius equation. Though extremely useful, this approximate solution assuming just one profile shape can never predict separation or any upstream influence. In contrast, in the LRHK method the integral forms of the momentum, moment of momentum and energy equations are solved using the Cohen-Reshotko family of boundary layer profiles. This method enables complete solutions of supersonic or hypersonic flow fields with embedded separated regions to be obtained. By iterating on the final conditions downstream of reattachment, a unique solution giving the separation and reattachment points can be found.

Short of solving the Navier-Stokes equations for the entire flow field, a task currently beyond the capacity of even the largest computer, the most accurate expression for δ^* is obtained by solving the boundary layer equations using one of the modern implicit finite difference schemes. Such schemes usually work well up to separation but cannot cope with separated flow. A notable exception is described in the paper by Flügge-Lotz and Reyhner⁽²⁰⁾, though they experienced considerable difficulty in calculating conditions within the separated zone and were forced to modify the boundary layer equations in order to obtain a stable solution in that region.

Turbulent flow

There are not many methods capable of predicting the growth of the hypersonic, non-adiabatic turbulent boundary layer in a strong pressure gradient. Even the most successful have to rely heavily on empirical relations and the use of Morkovins hypothesis. Many more comparisons between experiment and theory need to be made before confidence can be established though some methods begin to show great promise.^(21,22)

In contrast there are a number of relatively simple techniques for predicting flat plate flows as proposed by Spalding and Chi⁽²³⁾, Van Driest⁽²⁴⁾ and Eckert⁽²⁵⁾. Unfortunately, these theories can give estimates which differ by as much as 30% and the experimental data are so scattered that two recent reviews^(26,27) have inevitably led to two different suggestions as to which is the 'best' method. Until these difficulties are solved there is much to be said for using a simple theory especially when more involved flows have to be tackled.

One such complex flow is that past a compression corner. In our own tests Elfstrom⁽¹⁶⁾ noted and Coleman⁽²⁸⁾ has confirmed that the upstream influence of the corner is negligible until the incipient separation condition is reached. This suggests that a simple inviscid model⁽¹⁶⁾ may be useful for estimating the pressure distribution. Once this is known the heat transfer can be calculated using a 'local flat plate' method similar to that proposed by Walker.⁽²⁹⁾

The overall heat balance is satisfied by solving the energy integral equation

$$\frac{d}{dx} [\rho_b u_b (h_r - h_w) \phi] = \dot{q} \quad (5)$$

The local heat transfer rate (\dot{q}) is then expressed in terms of ϕ assuming local similarity, the simple power law relation for Stanton number and Eckert's reference enthalpy method to account for compressibility. The result is

$$\dot{q} = \frac{0.013 \rho_b u_b (h_r - h_w)}{Pr^{2/3}} \left\{ \frac{\rho^*}{\rho_b} \left(\frac{\mu^*}{\mu_b} \right)^{1/4} \right\} \left\{ \frac{h_r - h_w}{Pr^{2/3} H_0} \cdot \frac{\mu_b}{\rho_b u_b \phi} \right\}^{1/4} \quad (6)$$

Equations (5) and (6) may be combined and simplified to give

$$St = \frac{\dot{q}}{\rho_b u_b (h_r - h_w)} = \frac{0.0296 (\rho^*)^{4/5} (\mu^*)^{1/5}}{Pr^{2/3} (\rho_b) (\mu_b)} Re_X^{-1/5} \quad (7)$$

where

$$\rho_b u_b X = \int_0^x \rho_b u_b dx \quad (7a)$$

and x is measured from the virtual origin of the turbulent boundary layer. The success of these ideas is demonstrated later by comparison with experiment.

Results

Laminar flow

Figure 2 compares experimental data measured on sharp flat plates at zero and positive incidence with the Cheng and modified Cheng (MC) theories. Both agree reasonably well with the data though rarefied gas effects can cause the pressure to fall away near the leading edge as shown in Fig.2b. A further comparison is made in Figure 3 where the measurements of Allegre and Herpe⁽⁴⁷⁾ on a blunt plate at incidence are shown. Here the modified theory is the more accurate. For such simple flows there is no need to use a complex calculation method.

The prediction of flow over a concave surface is a more severe test of the theoretical methods and Figure 4 compares the data of Mohammadian⁽⁴⁵⁾ with various predictions. The oscillatory behaviour resulting from the use of Cheng's zero order theory is quite unrealistic and a more recent paper by Cheng and Kirsch⁽⁴⁶⁾ describes an improved solution. The modification suggested by Stollery gives a good estimate of the pressure distribution but under-values the heat transfer rate. The LRHK method on the other hand gives a better estimate of the heat transfer but the pressure is too high since the Prandtl-Meyer rule is used to describe the external inviscid flow. In fact a shock is formed by the compression process and the non-isentropic nature of the inviscid flow field must be allowed for if the theory is to be refined.

For the convex curved surface and the convex corner the external inviscid flow is isentropic and all the calculation methods give reasonable predictions (Fig.5). The heat transfer rate in Fig.5b has also been calculated using the finite-difference boundary-layer program of Sells⁽¹³⁾ with the measured pressure distribution as input. The agreement with experiment is good.

The most searching test of the theoretical methods is provided by flow past a deflected flap or compression corner. For attached flow, comparisons have been made with just two methods. Considering its simplicity the modified Cheng method is surprisingly good though inferior to the LRHK calculation. Beyond separation the LRHK method is the only accurate one and Fig.6 demonstrates its ability to calculate a fully separated flow. This method is also capable of predicting the incipient separation boundary and Fig.7 compares the results of such a 'computer experiment' with the wind tunnel data now available. Considering the assumptions in the theory and the difficulties in making the measurements the agreement is encouraging.

Turbulent flow

Flat plate. Flat plate heat transfer rate data¹⁵ at $M = 9$ are compared with some semi-empirical rules in Fig.8. The measurements are plotted against a Reynolds number based on the energy thickness (ϕ) obtained by integrating the measured heat transfer rate distribution from the leading edge, i.e.

$$\phi = \frac{\int_0^x \dot{q} dx}{\rho_\infty u_\infty (h_r - h_w)}$$

This avoids any difficulty associated with the choice of a virtual origin. In applying the various theories a Reynolds analogy factor of 1.0 has been used throughout. Whilst a somewhat higher value (e.g. 1.16) is favoured at supersonic speeds the recent measurements of Holden⁽³³⁾ suggest a lower figure for hypersonic cold-wall conditions. Figure 8 shows how the various estimates differ from each other and how many of them under-predict the measured heat transfer at low values of Re_ϕ . It seems that at hypersonic speeds the turbulent boundary layer takes a long time to reach its asymptotic or equilibrium form. The wake component is slow to develop so that at low Re_ϕ the profile is 'fuller' and the corresponding heat transfer rate is larger. Both Green⁽³⁰⁾ and Fernholz⁽³¹⁾ have attempted to allow for this profile variation.

Coleman has made some Preston tube measurements of skin friction coefficient to compare with his heat transfer data. Accepting the calibration of Keener and Hopkins⁽³²⁾ he obtains a Reynolds analogy factor of 0.85 which seems far too low. Table 1 compares the skin friction values derived from heat transfer measurements with various theoretical

TABLE 1 Estimates of skin friction coefficient

Case 1, $M_\infty = 8.96$, $T_w/T_0 = 0.28$, $Re_\infty = 0.12 \times 10^6/cm$ Natural transition, $Re_\theta = 3,300$		
Case 2, $M_\infty = 9.22$, $T_w/T_0 = 0.28$, $Re_\infty = 0.47 \times 10^6/cm$ Forced transition, $Re_\theta = 12,850$		
	1	2
	$C_f \times 10^3$	$C_f \times 10^3$
Coleman (\dot{q} , RAF = 1)	1.00	0.56
Coleman (\dot{q} , RAF = 1.16)	0.77	0.48
Sivasegarum	1.06	0.66
Van Driest II	0.96	0.69
Spalding-Chi	0.72	0.54
Fernholtz	0.99	0.60
Sommer-Short	0.85	0.61

estimates and with the value from the Clauser-type plot suggested by Sivasegarum⁽³⁴⁾ using the experimentally measured pitot-pressure profiles. Faced with such a variety of values it is impossible to know which is the correct result. The accurate measurement of skin friction remains one of the most difficult experimental tasks.

Compression corner. The results of the compression corner tests are shown in Fig.9. There are a number of striking features:

- (i) large flap deflections are needed to separate the turbulent boundary layer (typically 30° at $M=9$);
- (ii) prior to separation the upstream influence of the flap is very small (less than one boundary layer thickness);
- (iii) the heat transfer rate distribution non-dimensionalised by the flat plate value is very similar in form to the pressure distribution even in the separated flow regions where, in sharp contrast to laminar flow, the heat transfer rises.

This type of flow is a severe test for any theory and so far comparisons have only been made with some rather simple ideas. Because the turbulent Mach number profile is so 'full' a number of authors have suggested a pseudo-inviscid approach ignoring the laminar sub-layer. By suitable extrapolation of the 'shoulder' of the layer an 'inviscid' Mach number (M_w) at the wall is determined. The criterion for incipient separation is then postulated as the shock detachment condition for a wedge in a freestream M_w on the grounds that a normal shock is the most severe adverse pressure gradient possible. Elfstrom has shown that the criterion works well for $M \geq 3$ and has used the method to explain the diverse Reynolds number trends shown in Fig.10. At low Re_θ the wake component is developing, the profile becomes 'less full' and M_w decreases so that α_i falls with increasing Reynolds number. However, once the 'equilibrium profile' has developed it gradually grows fuller since the wall and wake components grow in different ways. (This is sometimes described by stating that n in $(u/u_1) = (y/\delta)^{1/n}$ increases with Re .) The result is that M_w and α_i then rise with increasing Reynolds number. To calculate the pressure distribution over the flap a simple inviscid, rotational characteristics scheme can be used, e.g. ref.16.

The heat transfer has been calculated using the variation of the local flat plate method described earlier. The reservoir pressure behind the oblique shock is calculated from tables. Given the (calculated) pressure distribution, the equivalent local Mach number and all other local freestream conditions are found assuming isentropic flow. Distance is measured along the surface from the effective origin of the turbulent boundary layer which was a point well ahead of the corner. The measured and calculated results are compared in Fig.11. Considering the simplicity of the calculation method the agreement is good.

Three-dimensional flow

Two-dimensional flows can be generated by three-dimensional shapes and the Nonweiler wing is a classical example. Townend et al.⁽³⁵⁾ have shown that such a vehicle designed for high incidence is very attractive for space shuttle applications.

However, most practical flows are more complex than those already considered. In order to assess the relevance of two-dimensional studies to a three-dimensional vehicle the windward flow on a flat-bottomed, sharp leading edge delta is being examined with and without a full span trailing edge flap. Rao⁽³⁶⁾ has measured the pressure distributions and overall forces. The heat transfer rate measurements are now being made. Rao showed that two-dimensional strip theory gave reasonable predictions for the pressure, provided the flow remained attached.

Figure 12 compares the incipient separation boundary with the two-dimensional data and shows two important differences. Firstly the flap angle for laminar incipient separation is increased on the delta wing. This is thought to be due to spanwise outflow at the hinge line which reduces the boundary layer thickness and inhibits separation. A similar effect is found when part span rather than full span flaps are used as shown on the figure. The second effect is the earlier rise of separation flap angle (α_i) with Reynolds number. This is due to transition and confirms the tests without flap which showed transition occurring on the delta wing at a lower Reynolds number than on the two-dimensional flat plate. Fully turbulent incipient separation on the delta wing agrees well with the two-dimensional data.

When the flow is separated there will be significant 3-D flow effects which no strip theory can describe. For example, Fig.13 shows the effect of Reynolds number on a well separated flow. At low Reynolds number a laminar separation occurs close to the leading edge and a 'conical' separation bubble covers nearly the whole of the undersurface of the wing with re-attachment on the trailing edge flap. As the Reynolds number is increased so the separation becomes transitional and the separated zone is diminished in extent. At the highest Reynolds number shown the flow on the centre line is turbulent and almost attached but in the more outboard regions near the tips the local Reynolds number is smaller, the flow transitional and the separated length is greater. A dumbbell-shaped separated zone is the result.

To return to a simpler flow, Fig.14 compares the heat transfer rate distribution over the lower surface of the unflapped delta wing with two-dimensional strip theory for laminar flow. At zero incidence the agreement between laminar theory and the measurements is good for all streamwise strips. At $\alpha = 10^\circ$ transition occurs first on the centre line but again the magnitude is fairly well predicted by strip theory. Further tests are now needed at higher incidences to see how far the concept of quasi-two-dimensional flow can be stretched.

Conclusions

There are now a number of methods with varying degrees of sophistication for calculating the growth of a laminar boundary layer, with and without viscous or shock-boundary layer interaction. The important parameters governing the effects of bluntness, displacement and shape are known and understood. Comparison between measurements and theory shows that the momentum integral technique is a very useful, powerful and accurate method

particularly for separated flows.

Turbulent boundary layer theory is not so well advanced. Reasonable predictions can be made for flat plate flow provided the slow development towards the equilibrium profile is allowed for. Viscous interaction is unlikely to be a problem and the turbulent layer is remarkably resistant to severe adverse pressure gradients. The pressure distribution and incipient separation can be predicted using simple inviscid ideas. When separation does occur it is accompanied by an increase in heat transfer rate in the separated region, a result in complete contrast to the laminar flow result.

Despite the complexity of many 3-D flows the results of 2-D flow can often be of value.

Acknowledgement

It gives me great pleasure to acknowledge the enthusiasm, effort and resource of the Research Students and Research Assistants pursuing hypersonic research at Imperial College. They have helped to provide much of the material in this paper.

Nomenclature

A	$\left(\frac{\gamma-1}{2}\right)0.664(1 + 2.6T_w/T_0)$
C	constant in temperature-viscosity law
C _f	skin friction coefficient
h	enthalpy
H ₀	total enthalpy
k	leading edge nose drag coefficient, $D_N/\frac{1}{2}\rho_\infty U_\infty^2 t$
L	distance to the hinge line
M	Mach number
p	pressure
P	p/p_∞
Pr	Prandtl number
\dot{q}	heat transfer rate
Re	Reynolds number
St	Stanton number
t	leading edge thickness
u, v	velocity components in the x and y directions
x, y	distance along and normal to the surface
X	defined by equation (7a)
α	wedge or flap angle
γ	ratio of the specific heats
δ^*	boundary layer displacement thickness
δ_e	entropy layer thickness
θ	momentum thickness
Λ	sweep back angle
μ	viscosity
ρ	density
ϕ	energy thickness
$\bar{\chi}$	the viscous interaction parameter, $M_\infty^3 \sqrt{C/Re_x}$

Suffices

b	edge of boundary layer (see Fig.1)	r	recovery
e	edge of equivalent body (see Fig.1)	w	wall
0	total	∞	freestream
		*	Eckert's reference enthalpy

References

1. CHENG, H.K., HALL, J.G., GOLIAN, T.C., and HERTZBERG, A., 'Boundary layer displacement and leading edge bluntness effects in high-temperature hypersonic flow', J. Aero Sci., 28, 353 (1961).
2. SULLIVAN, P.A., 'On the interaction of a laminar hypersonic boundary layer and a corner expansion wave', AIAA J., 8, 765 (1970).
3. STOLLERY, J.L., 'Hypersonic viscous interaction on curved surfaces', JFM, 43, 497 (1970).
4. STOLLERY, J.L., PIMPULKAR, S., and BATES, L., 'Hypersonic viscous interaction', Fluid Dynamics Transactions 6, part II, 545 (1971).
5. LEES, L., and REEVES, B.L., 'Supersonic separated and re-attaching laminar flows. 1 - General theory and application to adiabatic boundary layer/shock wave interactions', AIAA J., 2, 1907 (1964).
6. HOLDEN, M.S., 'Boundary layer displacement and leading edge bluntness effects on attached and separated laminar boundary layers in a compression corner. Part I: Theoretical study', AIAA J., 8, 2179 (1970). Part II: Experimental study, AIAA J., 9, 84 (1971).
7. KLINEBERG, J.M., and LEES, L., 'Theory of laminar viscous-inviscid interactions in supersonic flow', AIAA J., 7, 2211 (1969).
8. GEORGEFF, M.P., 'A comparison of integral methods for the prediction of laminar boundary layer - shock wave interaction', Imperial College Aero Report 72-01 (1972).
9. GEORGEFF, M.P., 'An extension of the Lees-Reeves-Klineberg method to two and three-dimensional boundary layers with arbitrary wall cooling ratio', Imperial College Aero Report 72-03 (1972).
10. WORNOM, S.F., and WERLE, M.J., 'Displacement interaction and surface curvature effects on hypersonic boundary layers', AIAA Paper 72- (1972).
11. FLÜGGE-LOTZ, I., and BLOTTNER, F.G., 'Computation of the compressible laminar boundary layer flow including displacement thickness interaction using finite-difference methods', Division of Engineering Mechanics, Stanford Univ. Tech. Rep. No.131 (1962).
12. DAVIS, R.T., 'Numerical solution of the hypersonic viscous shock layer equations', AIAA J., 8, 843 (1970).
13. SELLS, C.C.L., 'Two-dimensional laminar compressible boundary layer programme for a perfect gas', R&M 3533 (1968).
14. NEEDHAM, D.A., ELFSTROM, G.M., and STOLLERY, J.L., 'Design and operation of the Imperial College No.2 hypersonic gun tunnel', Imperial College Aero Report 70-04 (1970).
15. COLEMAN, G.T., 'Tabulated heat transfer rate data for a hypersonic turbulent boundary layer over a flat plate', Imperial College Aero Report 72-06 (1972).
16. ELFSTROM, G.M., 'Turbulent hypersonic flow at a wedge compression corner', JFM 53, 113 (1972).
17. CRABTREE, L.F., DOMMETT, R.L., and WOODLEY, J.G., 'Estimation of heat transfer to flat plates, cones and blunt bodies', RAE TR 65137 (1965).
18. CHERNYI, G.G., 'Introduction to hypersonic flow', Academic Press, New York.
19. LEES, L., 'Laminar heat transfer over blunt nosed bodies at hypersonic flight speeds', Jet Propulsion, 26, 259 (1956).
20. REYHNER, T.A., and FLÜGGE-LOTZ, I., 'The interaction of a shock wave with a laminar boundary

- layer', *Int. J. Non-linear Mechanics*, 3, 173 (1968).
- 21a ANDERSON, E.C., and LEWIS, C.H., 'Laminar or turbulent boundary-layer flows of perfect gases or reacting gas mixtures in chemical equilibrium', NASA CR-1893 (1971).
 - 21b KUHN, G.D., 'Calculation of compressible non-adiabatic boundary layers in laminar, transitional and turbulent flow by the method of integral relations', NASA CR-1797 (1971).
 22. PATANKAR, S.V., and SPALDING, D.B., 'Heat and mass transfer in boundary layers', Intertext, London, 2nd ed. (1970).
 23. SPALDING, D.B., and CHI, S.W., 'The drag of a compressible turbulent boundary layer on a smooth flat plate with and without heat transfer', *JFM* 18, p 117 (1964).
 24. VAN DRIEST, E.R., 'Problem of aerodynamic heating', *Aeronautical Engineering Review*, 15, p 26 (1956).
 25. ECKERT, E.R.G., 'Engineering relations for friction and heat transfer to surfaces in high velocity flow', *J. Aero. Sci.* 22, 585 (1955).
 26. HOPKINS, E.J., and INOUE, M., 'An evaluation of theories for predicting turbulent skin friction and heat transfer on flat plates at supersonic and hypersonic Mach numbers', *AIAA J.* 9, 993 (1971).
 27. CARY, A.M., 'Turbulent boundary-layer heat transfer and transition measurements for cold-wall conditions of Mach 6', *AIAA J.*, 6, 958 (1968).
 28. COLEMAN, G.T., and STOLLERY, J.L., 'Heat transfer in hypersonic turbulent separated flow', Imperial College Aero Report 72-05 (1972).
 29. WALKER, G.K., 'A particular solution to the turbulent boundary layer equations', *J. Aero. Sci.*, 27, 715 (1960).
 30. GREEN, J.E., 'A note on the turbulent boundary layer at low Reynolds number in compressible flow at constant pressure', RAE report (to be published).
 31. FERNHOLZ, H., 'Ein halbempirisches Gesetz für die Wandreibung in kompressiblen turbulenten Grenzschichten bei isothermer und adiabater Wand', *ZAMM*, 51, T 146-T 147 (1971).
 32. KEENER, E.R., and HOPKINS, E.J., 'Use of Preston tubes for measuring hypersonic turbulent skin friction', NASA TN D5544 (1969).
 33. HOLDEN, M.S., 'Shock wave-turbulent boundary layer interaction in hypersonic flow', *AIAA Paper No.72-74* (1972).
 34. SIVASEGARUM, S., 'The evaluation of local skin friction in compressible flow', *Roy. Aero. Soc. Aero J.* 75, 793 (1971).
 35. DAVIES, L., ROE, P.L., STOLLERY, J.L., and TOWNEND, L.H., 'Configuration design for high lift re-entry', RAE TM Aero 1379 (1971), also presented as *AIAA Paper No.*
 36. RAO, D.M., 'Hypersonic control effectiveness studies on delta wings with trailing edge flaps', Ph.D. Thesis, University of London (1970).
 37. APPELS, C., and BACKX, E., 'Hypersonic turbulent separated flow', VKI student report (1971).
 38. DROUGGE, G., 'An experimental investigation of the influence of strong adverse pressure gradients on turbulent boundary layers at supersonic speeds', *Proc. 8th Int. Cong. on Theoretical & Appl. Mech.*, Istanbul (1952), also *FFA Rep.* 46 (1953).
 39. GRAY, J.D., and RHUDY, R.W., 'Investigation of flat plate aspect ratio effects on ramp induced, adiabatic boundary layer separation at supersonic and hypersonic speeds', *AEDC-TR-70-235* (1971).
 40. KESSLER, W.C., REILLY, J.F., and MOCKAPETRIS, L.J., 'Supersonic turbulent boundary layer interaction with an expansion ramp and compression corner', McDonnell Douglas report MDC EO264 (1970).
 41. KUEHN, D.M., 'Experimental investigation of the pressure rise required for the incipient separation of turbulent boundary layers in two-dimensional supersonic flow', *NASA Memo* 1-2159A (1959).
 42. SPAID, F.W., and FRISHETT, J.C., 'Incipient separation of a supersonic turbulent boundary layer including the effects of heat transfer', *AIAA Paper* (Nov. 1971).
 43. STERRETT, J.R., and EMERY, J.C., 'Experimental separation studies for two-dimensional wedges and curved surfaces at Mach numbers of 4.8 to 6.2', *NASA TN D-1014* (1962).
 44. ROSHKO, A., and THOMKE, G.J., 'Supersonic turbulent boundary layer interaction with a compression corner at very high Reynolds numbers', *Proc. Symposium on Viscous Interaction Phenomena in Supersonic & Hypersonic Flow*, University of Dayton Press (1969).
 45. MOHAMMADIAN, S., 'Hypersonic boundary layers in strong pressure gradients', University of London Ph.D. thesis (1970). To be published in *JFM* (1972).
 46. CHENG, H.K., and KIRSCH, J.W., 'On the gas dynamics of an intense explosion with an expanding contact surface', *JFM* 39, 289 (1969).
 47. ALLEGRE, J., and HERPE, G., 'Effets d'incidence et d'émoussement sur les caractéristiques aérodynamiques d'une plaque plane en régime de forte interaction', *CNRS Report No.70-4* (1970).
 48. BALL, K.O.W., and KORKEGI, R.H., 'An investigation of the effect of suction on hypersonic laminar boundary layer separation', *AIAA J.*, 6, 239 (1968).
 49. NEEDHAM, D.A., 'Laminar separation in hypersonic flow', Ph.D. thesis, University of London (1965). Also *AIAA J.*, 5, 2284 (1967).
 50. BLOY, A., Present paper and 'Hypersonic laminar boundary layer flow over sharp compression and expansion corners', University of London Ph.D. thesis (1972).
 51. NIELSEN, see Richards, B.E., and Enkenhus, K.R., 'Testing in the VKI longshot free piston tunnel', *AIAA J.*, 8, 1020 (1970).
 52. MILLER, D.S., HYMAN, R., and CHILDS, M.E., 'Mach 8 to 22 studies of separation due to deflected control surfaces', *AIAA J.*, 12, 312 (1964).
 53. HARVEY, W.D., 'Experimental investigation of laminar-flow separation on a flat plate induced by deflected trailing-edge flap at $M = 19$ ', *NASA TN D-4671* (1968).
 54. KEYES, J.W., 'Pressures and heat transfer on a 75° swept delta wing with trailing-edge flap at Mach 6 and angles of attack to 90° ', *NASA TN D-5418* (1969).
 55. DAVIES, L., et al., 'A comparison between free flight and balance measurements for a 76° swept delta with a full span trailing edge flap at hypersonic speed', RAE report to be published.
 56. PUTNAM, L.E., 'Investigation of effects of ramp span and deflection angle on laminar boundary layer separation at Mach 10.03', *NASA TN D-2833* (1965).
 57. HOLLOWAY, P.F., STERRETT, J.R., and CREEKMORE, H.S., 'An investigation of heat transfer within regions of separated flow at a Mach no. of 6', *NASA TN D-3074* (1965).
 58. JOHNSON, C.B., 'Pressure and flow field study at

M = 8 of flow separation on a flat plate with deflected trailing-edge flap', NASA TN D-4308 (1968).

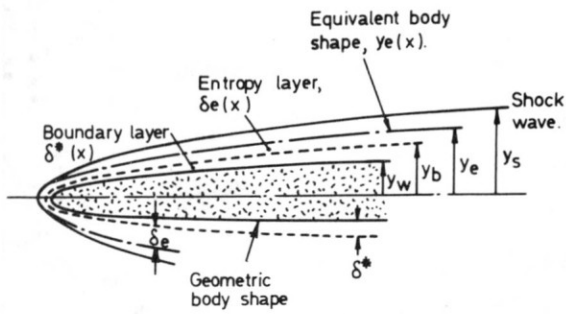


FIG. 1a HYPERSONIC VISCOUS FLOW PAST A BLUNT BODY.

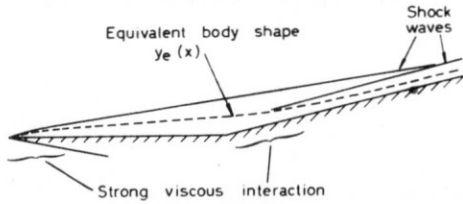


FIG. 1b HYPERSONIC VISCOUS FLOW PAST A SHARP EDGED FLAT PLATE WITH DEFLECTED TRAILING-EDGE CONTROL.

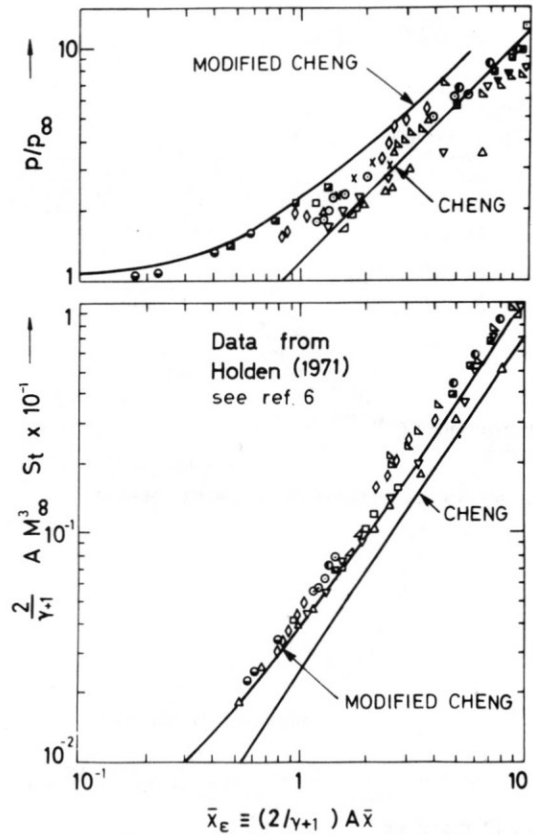


FIG. 2b CORRELATION OF PRESSURE AND HEAT TRANSFER DATA ON SHARP FLAT PLATES

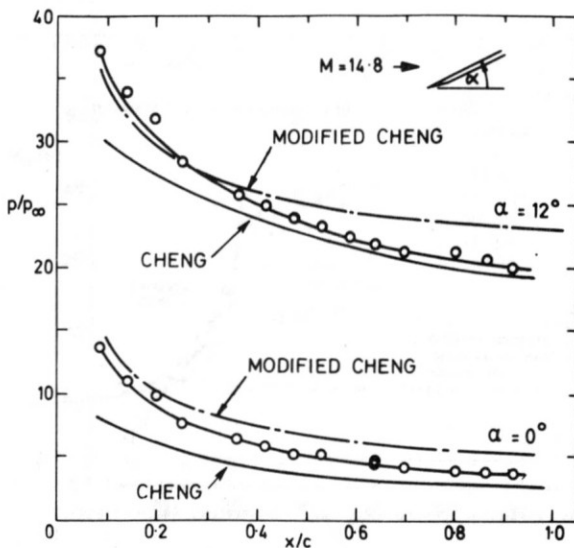


FIG. 2a PRESSURE DISTRIBUTION ON A SHARP FLAT PLATE. SOME COMPARISONS BETWEEN EXPERIMENT AND THEORY.

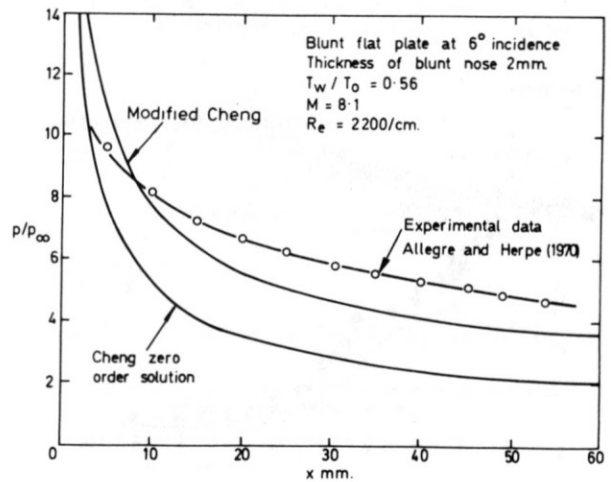


FIG. 3 COMPARISONS FOR A BLUNT FLAT PLATE AT ZERO AND POSITIVE INCIDENCE.

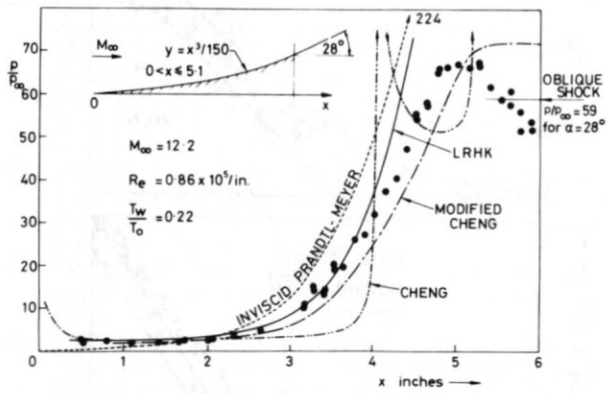


FIG 4a PRESSURE DISTRIBUTION ON A CONCAVE SURFACE.

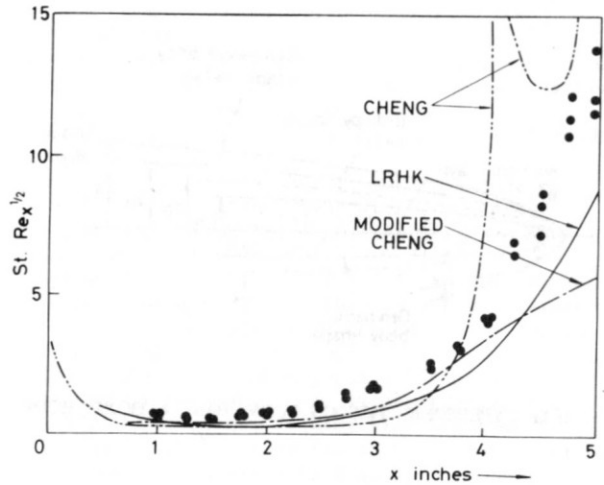


FIG 4b HEAT TRANSFER RATE DISTRIBUTION OVER THE CONCAVE SURFACE $y = x^2/150$.

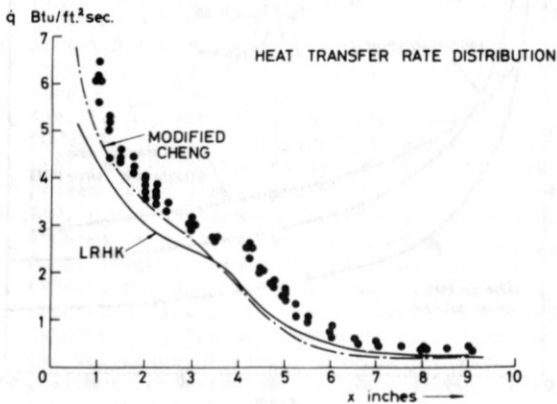
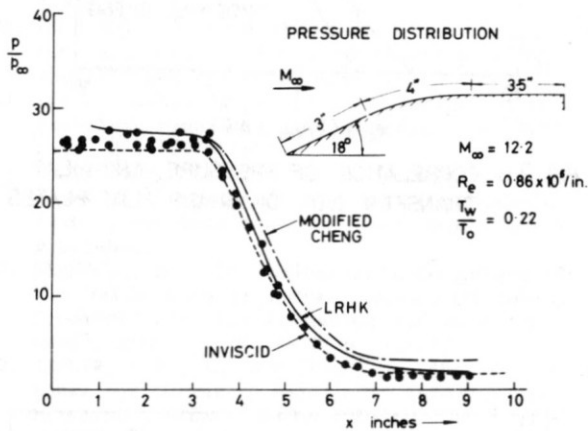


FIG 5a CONVEX SURFACE DATA AND COMPARISON WITH THEORY

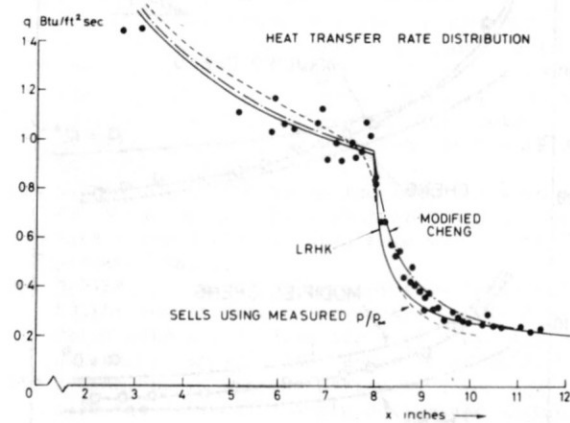
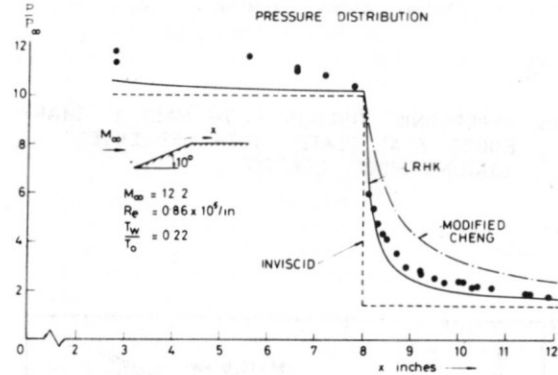


FIG 5b EXPANSION CORNER DATA AND COMPARISON WITH THEORY

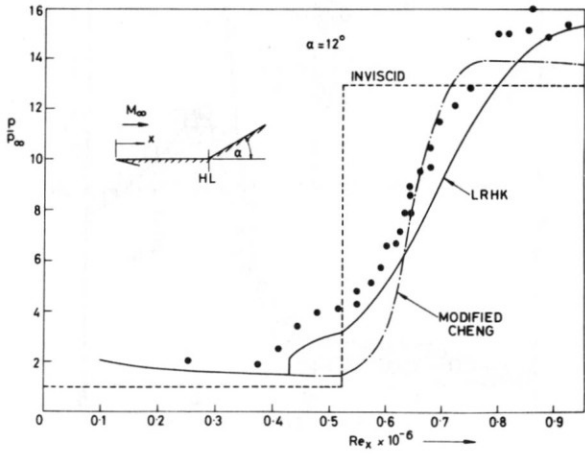
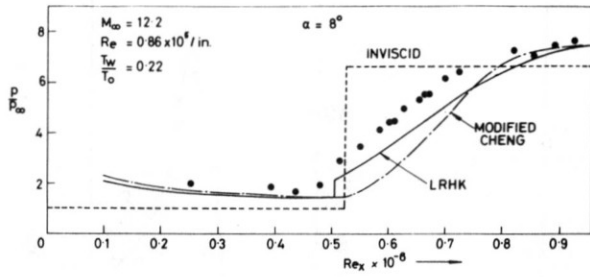


FIG. 6a COMPRESSION CORNER PRESSURE DATA AND COMPARISON WITH THEORY.

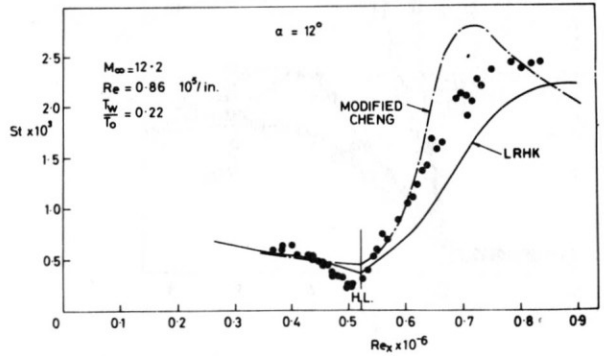
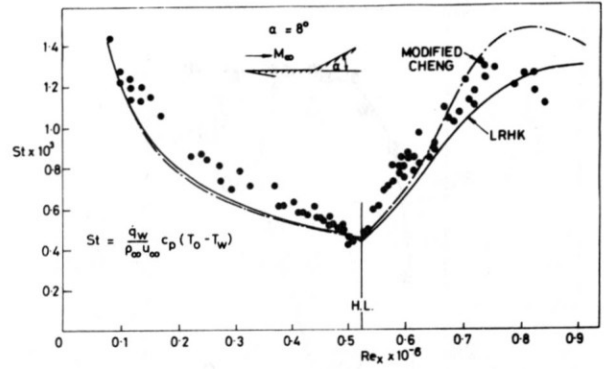


FIG. 6b COMPRESSION CORNER HEAT TRANSFER RATE DATA AND COMPARISON WITH THEORY.

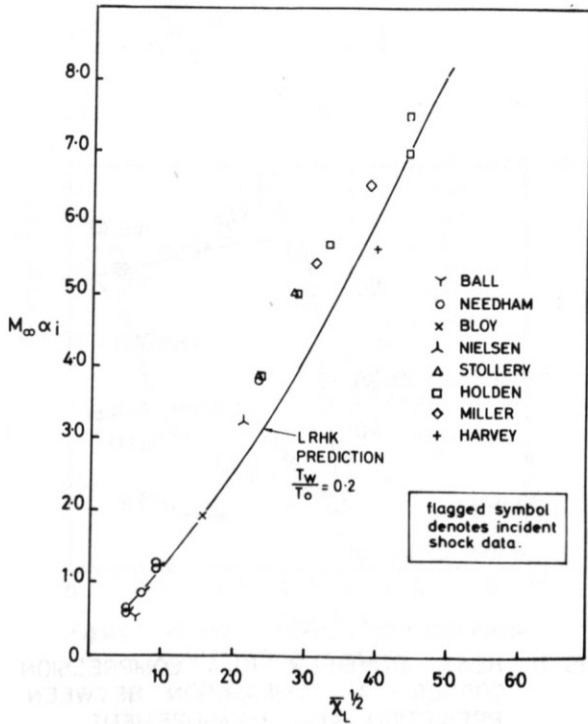


Fig. 7. LAMINAR, COLD-WALL, INCIPENT SEPARATION.

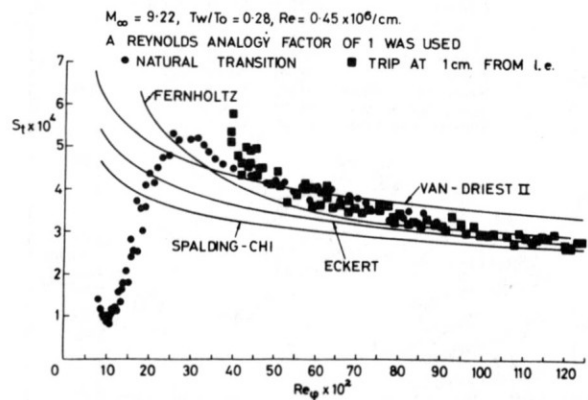


FIG. 8 FLAT PLATE HEAT TRANSFER - A COMPARISON BETWEEN EXPERIMENT AND THEORY AT $M_\infty = 9$.

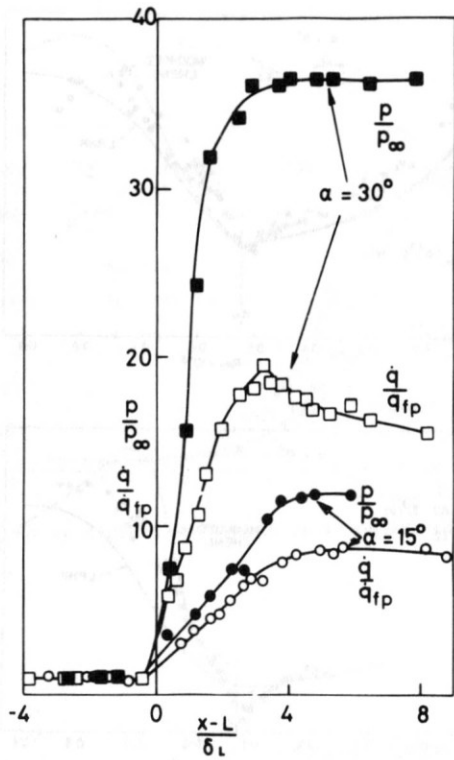


FIG. 9a PRESSURE AND HEAT TRANSFER RATE DISTRIBUTIONS ON A COMPRESSION CORNER MODEL $M_\infty = 9.22$, $Re = 0.47 \times 10^6/cm$, $T_w/T_o = 0.28$.

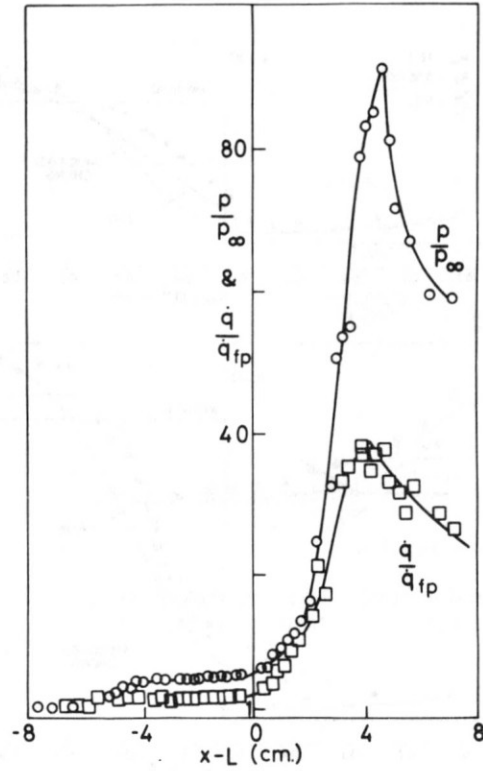


FIG. 9b PRESSURE AND HEAT TRANSFER RATE DISTRIBUTIONS ON A COMPRESSION CORNER MODEL, $\alpha = 38^\circ$, $M_\infty = 9.22$, $Re = 0.47 \times 10^6/cm$, $T_w/T_o = 0.28$.

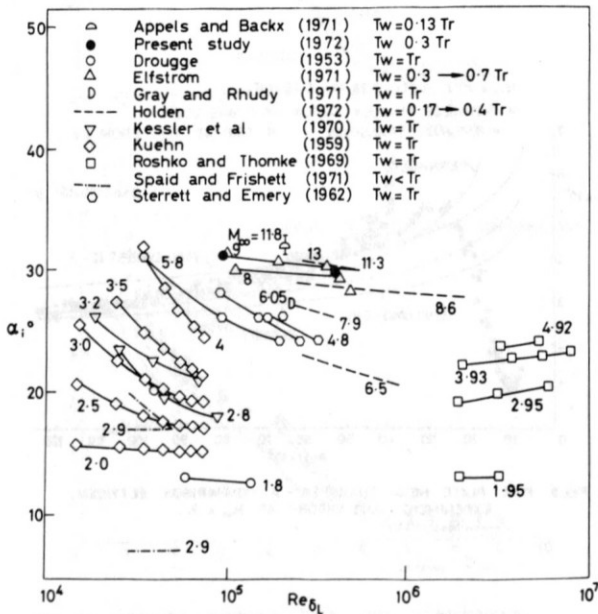


FIG. 10 INCIPIENT SEPARATION AT A WEDGE COMPRESSION CORNER, TURBULENT BOUNDARY LAYER.

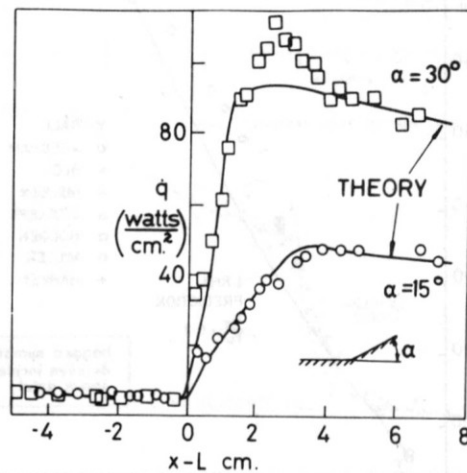


FIG. 11 HEAT TRANSFER TO A COMPRESSION CORNER - A COMPARISON BETWEEN PREDICTION AND MEASUREMENT. $M_\infty = 9.22$, $Re = 0.47 \times 10^6/cm$, $T_w/T_o = 0.28$

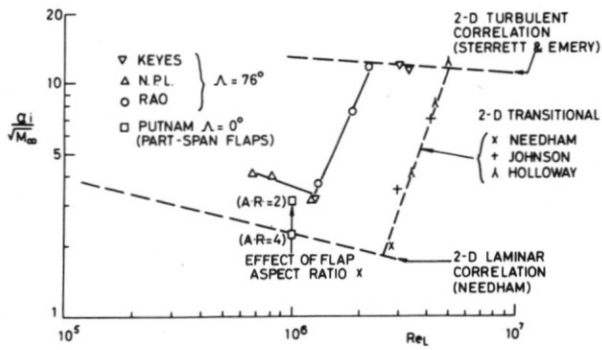


FIG. 12 INCIPIENT SEPARATION FOR 2D AND 3D FLOWS.

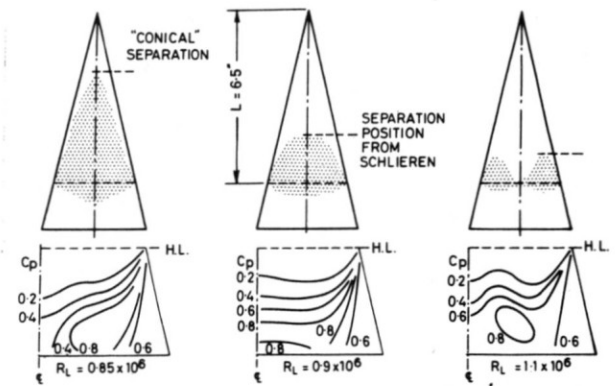


FIG. 13 REYNOLDS NO EFFECT ON FLOW OVER LOWER SURFACE OF A DELTA WING AT ZERO INCIDENCE. FLAP ANGLE = 30°

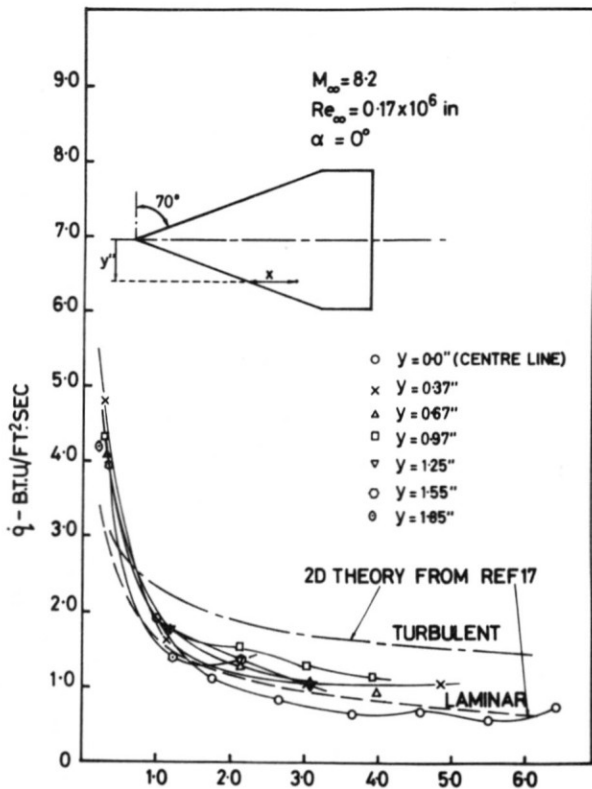


Fig.14a. DISTANCE PARALLEL TO FLOW FROM LEADING EDGE - X INCHES

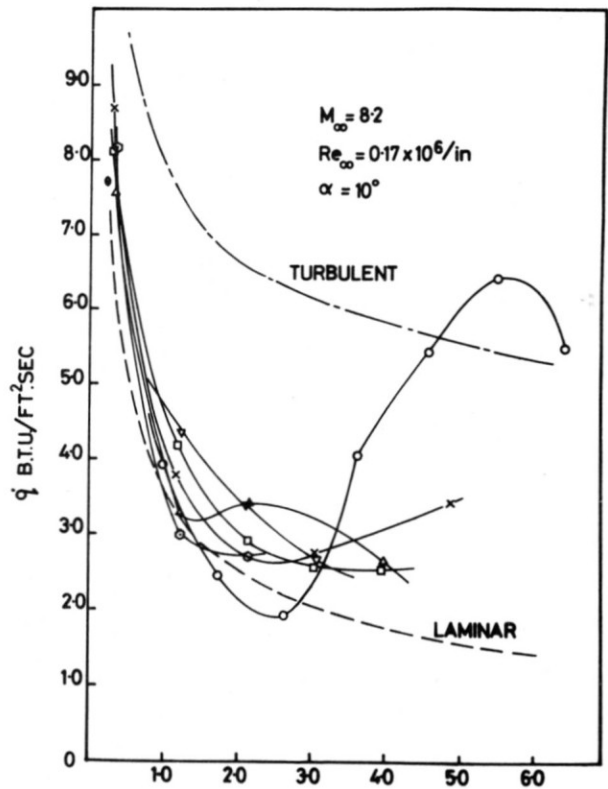


Fig.14b. DISTANCE PARALLEL TO FLOW FROM LEADING EDGE X-INCHES